

Type Ia Supernova Models and Progenitor Scenarios

Ken'ichi Nomoto^{1,†}, Yasuomi Kamiya^{2,1}, and Naohito Nakasato³

¹Kavli Institute for the Physics and Mathematics of the Universe, The University of Tokyo,
 5-1-5 Kashiwanoha, Kashiwa, Chiba 277-8583, Japan

²Department of Astronomy, Graduate School of Science, The University of Tokyo,
 7-3-1 Hongo, Bunkyo-ku, Tokyo 113-0033, Japan

³Department of Computer Science and Engineering, University of Aizu,
 Aizu-Wakamatsu, Fukushima 965-8580, Japan

[†]email: nomoto@astron.s.u-tokyo.ac.jp

Abstract.

We review some recent developments in theoretical studies on the connection between the progenitor systems of Type Ia supernovae (SNe Ia) and the explosion mechanisms. (1) *DD-subCh*: In the merging of double C+O white dwarfs (DD scenario), if the carbon detonation is induced near the white dwarf (WD) surface in the early dynamical phase, it could result in the (effectively) sub-Chandrasekhar mass explosion. (2) *DD-Ch*: If no surface C-detonation is ignited, the WD could grow until the Chandrasekhar mass is reached, but the outcome depends on whether the quiescent carbon shell burning is ignited and burns C+O into O+Ne+Mg. (3) *SD-subCh*: In the single degenerate (SD) scenario, if the He shell-flashes grow strong to induce a He detonation, it leads to the sub-Chandra explosion. (4) *SD-Ch*: If the He-shell flashes are not strong enough, they still produce interesting amount of Si and S near the surface of C+O WD before the explosion. In the Chandra mass explosion, the central density is high enough to produce electron capture elements, e.g., stable ⁵⁸Ni. Observations of the emission lines of Ni in the nebular spectra provides useful diagnostics of the sub-Chandra vs. Chandra issue. The recent observations of relatively low velocity carbon near the surface of SNe Ia provide also interesting constraint on the explosion models.

Keywords. nucleosynthesis, supernova, white dwarf

1. Introduction

The observed features of Type Ia supernovae (SNe Ia) have been well-understood by a thermonuclear explosion of a carbon-oxygen (C+O) white dwarf (WD). Both the Chandrasekhar mass [*Chandra* (*Ch*) model] and the sub-Chandrasekhar mass [*sub-Chandra* (*subCh*) model] have been presented (e.g., Livio 2000). However, there has been no clear observational indication as to how the WD mass grows until carbon ignition; i.e., whether the WD accretes H/He-rich matter from its binary companion [*single degenerate* (*SD*) scenario], or two C+O WDs merge [*double degenerate* (*DD*) scenario] (e.g., Hillebrandt & Niemeyer 2000, Nomoto *et al.* 1997, 2000, 2009, Arnett 1996). Even before these issues are resolved, several candidates of *super-Chandrasekhar* mass explosions have been observed (e.g., Hachisu *et al.* 2012 and references therein).

Recent modeling shows that DD merging could result in both the Chandra and the (effectively) sub-Chandra explosions. The SD scenario could also result in both the Chandra and sub-Chandra explosions. Here we review such cross connections between (DD, SD) scenarios and (Chandra, sub-Chandra) models, and some observational constraints.

(1) *DD-subCh*: In the DD scenario, if the carbon detonation is induced near the WD

surface in the early dynamical phase, it could result in the (effectively) sub-Chandra explosion. (2) *DD-Ch*: If no detonation is induced, the WD could grow until the Chandrasekhar mass is reached. The outcome depends on whether the quiescent carbon shell-burning is ignited and burns interior C+O into O+Ne+Mg. (3) *SD-subCh*: In the SD scenario, if the He shell-flashes grow strong to induce a He detonation, it leads to the sub-Chandra explosion. (4) *SD-Ch*: If the He-shell flashes are not strong enough to induce a He detonation, such flashes produce interesting amount of intermediate mass elements, including Si and S, as unburned material near the surface of C+O WD.

2. C+O Double Degenerates to Sub-Chandra Mass Explosion

In the DD scenario (Iben & Tutukov 1984, Webbink 1984), two C+O WDs form a close binary system after the common envelope phase and get closer by losing orbital angular momentum due to gravitational radiation. Eventually, the less massive WD with a mass M_2 fills its Roche lobe and dynamically evolves into the formation of a massive disk/envelope around the more massive WD with a mass M_1 .

Such a dynamical evolution of WD binary has been studied by number of authors (Benz *et al.* 1990, Segretain *et al.* 1997, Guerrero *et al.* 2004, Shioya *et al.* 2007, Pakmor *et al.* 2010) using the Smoothed Particle Hydrodynamics (SPH) method.

Surface Carbon Detonation: The important question is whether the merging process ignites a surface carbon detonation in the WD. During the early merging process, the shock heating increases the temperature in the surface C+O layer of the primary (i.e., more massive) WD. If the temperature becomes high enough to induce C-detonation (Pakmor *et al.* 2010 adopted the critical temperature of 2.5×10^9 K), the detonation wave propagates through the central region of the primary WD. Eventually, the whole primary WD is detonated and disrupted.

This model is essentially the sub-Chandra mass explosion, because the detonated WD has a sub-Chandra mass of $M_1 = 0.9\text{--}1.1M_\odot$ and the central density is as low as $\sim 10^7$ g cm $^{-3}$ (Pakmor *et al.* 2010, 2011). The explosion produce a larger amount of ^{56}Ni for larger M_1 .

3. Double Degenerates to Chandra Mass Explosion or Collapse

Suppose the surface C-detonation is not triggered in the early dynamical phase of merging. Then the next important question is whether the merging process ignites not the C-detonation but “quiescent” off-center carbon burning in the WD. Once carbon is ignited, carbon flame moves inward by heat conduction to reach the center (Saio & Nomoto 1985, 1998). The released nuclear energy is lost in neutrinos, and the C+O WD is converted into the O+Ne+Mg WD non-explosively. The ONeMg WDs eventually collapse due to electron capture rather than exploding as SNe Ia (Nomoto 1984, 1987).

3.1. Carbon Shell Burning and Chandra Explosion or Collapse

Here the carbon ignition temperature T_{ign} is defined by $\epsilon_{\text{C+C}} = \epsilon_\nu$, where $\epsilon_{\text{C+C}}$ and ϵ_ν denote the nuclear energy generation rate and the neutrino energy loss rate, respectively. At $\rho \sim 1\text{--}3 \times 10^6$ g cm $^{-3}$, $T_{\text{ign}} \sim 6 \times 10^8$ K (Nomoto & Iben 1985, Kawai *et al.* 1987, Yoon *et al.* 2007).

For $T > T_{\text{ign}}$, $\epsilon_{\text{C+C}} > \epsilon_\nu$ and the carbon flash is ignited, and the conductive carbon flame propagates inward. If $T < T_{\text{ign}}$, on the contrary, $\epsilon_{\text{C+C}} < \epsilon_\nu$ and the neutrino cooling dominates to induce the gradual contraction of the C-rich envelope. Then carbon flame is not formed.

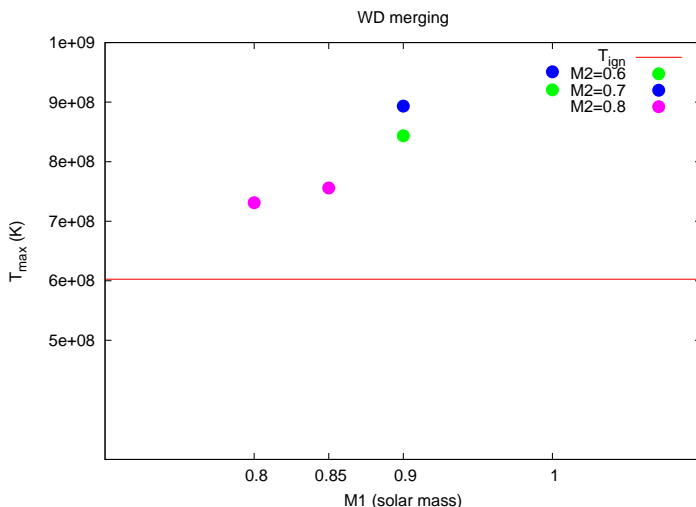


Figure 1. The local peak temperature T_{peak} attained 2.5 min after the start of merging of double C+O white dwarfs with masses (M_1, M_2) (Nakasato & Nomoto 2011). For $T_{\text{peak}} > T_{\text{ign}}$, off-center carbon burning is ignited.

There are two possible cases for the off-center carbon ignition to occur.

Case 1: When the falling materials from the less massive star compress the outer layer of the more massive star, the material could be heated up to high enough temperature to ignite carbon burning.

Case 2: Later, if the accretion rate exceeds a critical rate of $2.7 \times 10^{-6} M_{\odot} \text{ yr}^{-1}$, compressional heating exceeds radiative cooling and leads to carbon ignition (Nomoto & Iben 1985, Kawai *et al.* 1987).

For Case 1, Yoon *et al.* (2007) calculated the merging process until 5 min after its start and showed that a quasi-static equilibrium configuration is reached consisting of a cold core, hot envelope, and a disk. The peak temperature T_{peak} reaches a stationary value. For $M_1 = 0.9 M_{\odot}$ and $M_2 = 0.6 M_{\odot}$, T_{peak} is marginally lower than T_{ign} . Whether the later off-center carbon ignition of Case 2 takes place depends on the effective accretion rate, which needs further study (e.g., Shioya *et al.* 2007, Shen *et al.* 2012).

For Case 1, Nakasato & Nomoto (2011) have recently conducted the SPH simulation (Nakasato & Nomoto 2003) with the number of particles $N = 300,000$ and $N = 1,000,000$ for various combinations of (M_1, M_2) . The artificial viscosity is treated to minimize numerical effects according to the hybrid scheme proposed by Rosswog *et al.* (2010). The Helmholtz equation of state is used (Timmes & Swesty 2000), and the WD is assumed to be composed of 50 % of carbon and 50 % of oxygen.

The local peak temperatures shown in Figure 1 are obtained from particles at $\rho \sim 1 - 3 \times 10^6 \text{ g cm}^{-3}$ at 2.5 min after the start of merging. T_{peak} has already reached its stationary value, which is confirmed with some test runs calculated until 10 min after the merging. It is seen that T_{peak} is determined mainly by M_1 with small dependence on M_2 . This implies that the gravitational potential of the more massive WD is the main factor to determine T_{peak} .

Figure 1 shows that $T_{\text{peak}} > T_{\text{ign}}$ for most cases of (M_1, M_2) . Thus carbon flash will take place to form a carbon flame that propagates inward to convert C+O into O+Ne+Mg.

How the above results depend on the set-up of the merging calculations (Dan *et al.* 2011)?

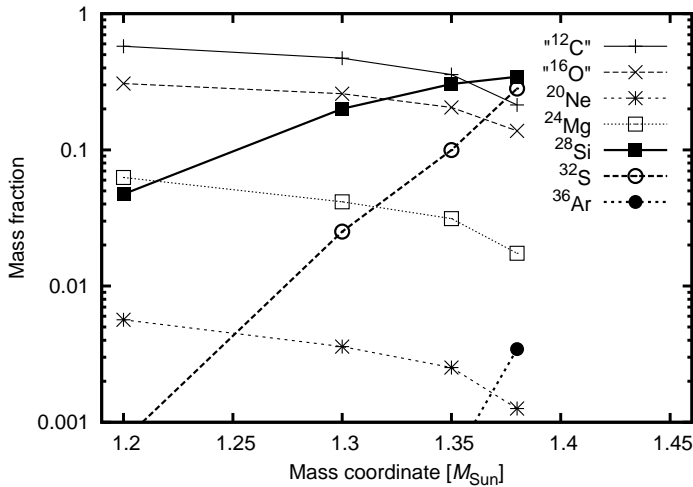


Figure 2. Abundance distribution of the products of He shell flashes in an accreting WD just before the explosion (Kamiya & Nomoto 2011).

The initial separation is set to be $a = (0.9R_2)/r_L$ where R_2 is the radius of the less massive WD and r_L is the effective Roche lobe radius. Some test runs adopting a larger separation confirm that T_{peak} is not sensitive to the initial separation.

Comparisons between the runs with $N = 300,000$ and with $N = 1,000,000$ show that T_{peak} of the higher resolution run is always slightly higher than the low resolution run. Thus carbon ignition of Case 1 is quite likely for most cases of (M_1, M_2) .

3.2. Further Evolution of Rotating White Dwarfs

The WD formed from merging must be rapidly rotating. The “SN Ia mass” of the WD with which SN Ia is triggered is $M_{\text{Ia}} = 1.48M_\odot$ for a uniformly rotating WD at the critical rotation (Uenishi *et al.* 2003). This is larger than $1.38M_\odot$ for the non-rotating WD. For non-uniform, differentially rotating WDs, M_{Ia} is as large as $\gtrsim 2M_\odot$ (Yoon & Langer 2004, Hachisu *et al.* 2012). Therefore, even if no carbon flame is formed, the WD may not reach M_{Ia} because of some mass loss after merging.

4. Single Degenerate to Sub-Chandra Explosion

In the SD scenario, H-burning produces a thin He layer, and He-flashes are ignited when the He mass reaches a certain critical value. The strength depends on the He envelope mass M_{env} , thus depending on the accretion rate.

The He envelope mass M_{env} is larger for the slower mass-accumulation rate of the He layer \dot{M}_{He} . For $\dot{M}_{\text{He}} \gtrsim 1 \times 10^{-8} M_\odot \text{ yr}^{-1}$, M_{env} exceeds a critical value where the density at its bottom becomes high enough to induce a He detonation. This would result in the sub-Chandra explosion (e.g., S. Sim in this conference).

5. Single Degenerate to Chandra Mass Explosion

For higher \dot{M}_{He} , the He-shell flashes are not strong enough to induce a He detonation. Then, such flashes repeat many times with the increasing WD mass M_{WD} toward the Chandrasekhar mass. Kamiya & Nomoto (2011) calculated nucleosynthesis in such He shell flashes for various set of $(M_{\text{WD}}, M_{\text{env}})$ (see also Shen & Bildsten 2007).

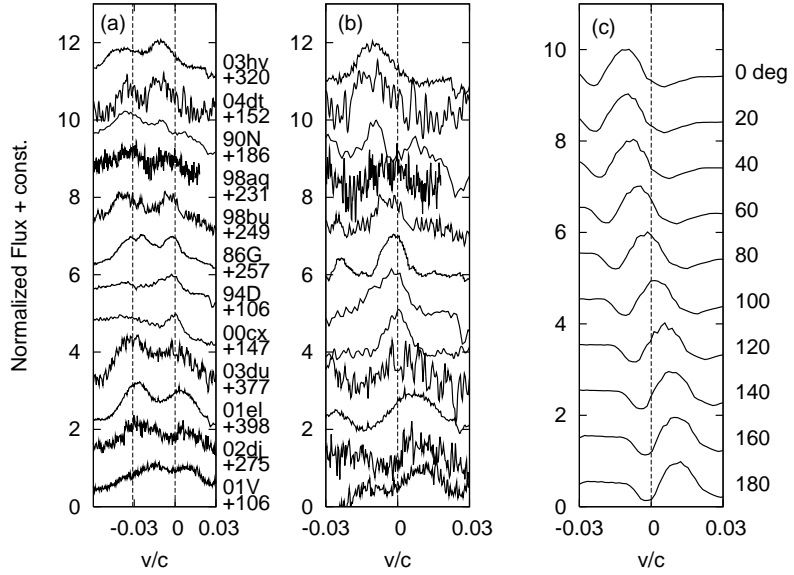


Figure 3. Analysis of the [Ni II] $\lambda 7378$ line profiles in 12 SNe Ia (Maeda *et al.* 2010a). The velocity is set assuming that the rest wavelength is at 7378 \AA . (a) Observed line profiles. The rest wavelengths of [Fe II] $\lambda 7155$ and [Ni II] $\lambda 7378$ are shown by dotted lines. (b) [Ni II] $\lambda 7378$ in observations, after removing the underlying continuum (or possible other lines). (c) Synthetic line profiles of the [Ni II], depending on the viewing orientation.

For $\dot{M}_{\text{He}} \sim (0.5 - 1) \times 10^{-7} M_{\odot} \text{ yr}^{-1}$, the WD is expected to undergo He shell-flashes at $(M_{\text{WD}}/M_{\odot}, \log(M_{\text{env}}/M_{\odot})) \sim (1.2, -2.5), (1.3, -3), (1.35, -3.5), (1.38, -4)$ as M_{WD} grows (Kato *et al.* 2008).

In the early stages of the He shell-flash, the envelope is electron-degenerate and geometrically almost flat. Thus the temperature at the bottom of the He-burning shell increases because of the almost constant pressure there. Heated by nuclear burning, the helium envelope gradually expands, which decreases the pressure. Then, the temperature attains its maximum and starts decreasing. The maximum temperature is higher for more massive WD and more massive envelope because of higher pressure.

For higher maximum temperatures, heavier elements, such as ^{28}Si and ^{32}S , are synthesized. However, the maximum temperature is not high enough to produce ^{40}Ca . After the peak, some amount of He remains unburned in the flash and burns into C+O during the stable He shell burning.

In this way, it is possible that interesting amount of intermediate mass elements, including Si and S, already exist in the unburned C+O layer at $M_r \geq 1.2M_{\odot}$. Such a distribution is shown in Figure 2 for $\dot{M}_{\text{He}} \sim 5 \times 10^{-8} M_{\odot} \text{ yr}^{-1}$. A part of them might be ejected out. Therefore the above quantity of the synthesized elements are overestimated.

6. Electron Capture in Chandra Mass Models

Both Chandra and sub-Chandra explosion models can synthesize relevant amount of ^{56}Ni for SNe Ia. However, the amount of other Fe-peak elements differs, because the ignition density is different, being as high as $> 10^9 \text{ g cm}^{-3}$ in the Chandra model, while as low as $\sim 10^7 \text{ g cm}^{-3}$ in the sub-Chandra model.

In the Chandra model, the thermonuclear runaway starts with the ignition of defla-

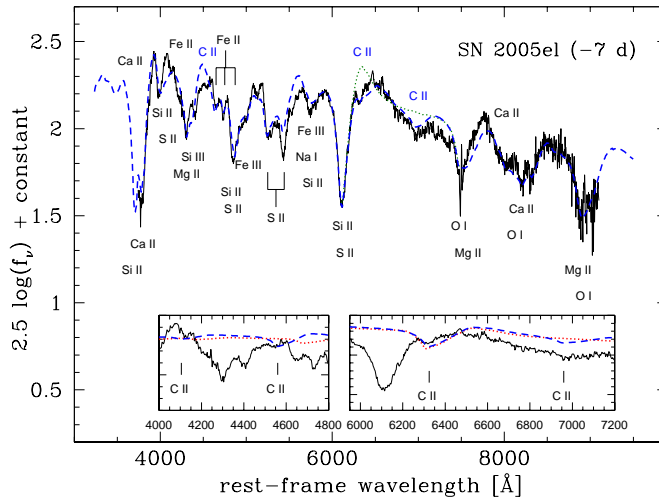


Figure 4. Spectrum of SN 2005el at -7 days (*solid line*), and a matching SYNOW calculation (*dashed line*). (*Insets*) The spectrum near the location of C II lines (*solid line*), the SYNOW spectra containing only C II (*dashed line*), and only H I (*dotted line*). The expected locations of C II lines are marked (Folatelli *et al.* 2012)

gration (e.g., Nomoto *et al.* 1976, 1984). In the high temperature and density bubble, materials are incinerated into NSE (nuclear statistical equilibrium) and undergo electron capture. Electron capture on free protons and Fe-peak elements leads to the synthesis of ^{58}Ni , ^{54}Fe , and ^{56}Fe (not via ^{56}Ni decay). These neutron-rich Fe-peak elements form an almost ^{56}Ni -empty hole (e.g., Nomoto *et al.* 1984).

In the sub-Chandra model, the ignition density is too low for electron capture to take place. The neutron excess is produced only by the initial CNO elements which are converted to ^{14}N and to ^{22}Ne , thus depending on the initial metallicity. As a result, the mass fraction of ^{58}Ni is as small as ~ 0.01 (e.g., Shigeyama *et al.* 1992).

Such a difference in the amount of ^{58}Ni can be observationally investigated by late-phase (~ 1 yr since the explosion) spectroscopy at near-infrared (NIR) wavelength. Because the ejecta become optically thin in late phases, spectroscopy provides an unbiased, direct view of the innermost regions.

Figure 3 shows the spectral feature around $\sim 7000 - 7500 \text{ \AA}$, i.e., $[\text{Fe II}] \lambda 7155$ (with some contribution from $[\text{Fe II}] \lambda 7171$) and $[\text{Ni II}] \lambda 7378$, for 12 SNe Ia (Maeda *et al.* 2010a). The $[\text{Ni II}] \lambda 7378$ line is emitted from the electron capture region of the ejecta, which is supported by the relatively narrow width ($\lesssim 3,000 \text{ km s}^{-1}$) of the $[\text{Ni II}]$ line. Thus the existence of $[\text{Ni II}]$ line implies the ignition at high density, thus favoring the Chandra model.

It is also interesting to note that these emission lines show the velocity shift, which indicates the off-center ignition and aspherical nature of SN Ia explosions (Maeda *et al.* 2010a, 2010b). The aspherical features could be seen in the light echo from Tycho’s supernova remnant (Usuda *et al.* 2011).

7. Carbon in SNe Ia

Parrent *et al.* (2011) and Folatelli *et al.* (2012) investigated the presence of unburned material in early-time spectra of SNe Ia. They find that at least 30% of the objects in the sample show absorption at about 6300 \AA which can be associated with C II $\lambda 6580$

(Figure 4). This would imply a larger incidence of carbon in SN Ia ejecta than previously noted. If confirmed as carbon, the material producing the observed features would be present at very low expansion velocities, merely $\sim 1,000 \text{ km s}^{-1}$ above the Si II velocities.

Carbon must be present in very deep regions, corresponding to velocities as low as $v \approx 11,000 \text{ km s}^{-1}$. This is well below the expected limit imposed by one-dimensional models, and points directly to large mixing effects and/or possible departures from spherical symmetry or clumpiness.

In spherically symmetric models, irrespective of the details of the flame propagation (deflagration or detonation), the production of a large amount of ^{56}Ni ($\sim 0.6M_{\odot}$) requires that the strength of the flame, which must lead to the total consumption of carbon below $15,000 - 20,000 \text{ km s}^{-1}$ (Nomoto *et al.* 1984, Shigeyama *et al.* 1992, Iwamoto *et al.* 1999). The situation is different for non-spherical models. For example, the off-center ignition model (Maeda *et al.* 2010a; see also Kasen *et al.* 2009) synthesizes $0.54M_{\odot}$ of ^{56}Ni and carbon with a mass fraction of ~ 0.1 at velocities as low as $\sim 13,000 \text{ km s}^{-1}$. This is still larger than the observed velocity, but suggests that the non-spherical effects may be important to understand the detection of carbon deep in the ejecta.

The existence of carbon at relatively low velocity suggests the presence of fair amount of unburned C+O materials. The amount Fe peak elements in such an unburned layer depends on the metallicity. Further observations of early UV spectra could show significant metallicity effects.

8. Concluding Remarks

As summarized above, recent modeling shows that DD merging could result in both the Chandra and the sub-Chandra explosions depending on whether a carbon detonation is induced near the surface of more massive WD. The SD scenario could also result in both the Chandra and sub-Chandra explosions depending on whether the He shell-flashes near the surface of the WD induce a He detonation.

- For DD-subCh, it is critically important to confirm the formation of surface carbon detonation by means of 3D hydrodynamical simulations rather than SPH method.
- For DD-Ch, whether carbon ignition can occur for both Case 1 and Case 2 needs further study for various set of (M_1, M_2) .
- For SD-subCh, a mechanism to avoid the production of too much ^{56}Ni in the surface should be studied. In case of the He-WD and C-WD merger, formation of an extended He envelope needs to be avoided.
- For SD-Ch, the outcome of quiescent He-shell flashes, e.g., nucleosynthesis, the rate of the He wind mass loss, needs to be studied.
- Finally, detailed hydrodynamical modeling of the WD spin-down is necessary. In this spin-down scenario (e.g., Justham 2011, Di Stefano *et al.* 2011, Ilkov & Soker 2012, Hachisu *et al.* 2012), an almost uniformly rotating C+O WD with a mass range of $1.38 - 1.48 M_{\odot}$ forms and eventually contract to ignite carbon after a long spin-down time. The outcome depends on the ignition density. If it is as high as $\sim 10^{10} \text{ g cm}^{-3}$, electron capture induces collapse rather than explosion (Nomoto & Kondo 1991). If it is lower, an SN Ia explosion would result.

This research has been supported in part by World Premier International Research Center Initiative, MEXT, Japan, and by the Grant-in-Aid for Scientific Research of the JSPS (23540262) and MEXT (22012003, 23105705).

References

- Arnett, W.D. 1996, *Nucleosynthesis and Supernovae* (Princeton: Princeton Univ. Press)
- Benz, A.O., Cameron, A.G.W., Press, W.H., & Bowers, R.L. 1990, *ApJ*, 348, 647
- Dan, M., Rosswog, S., Guillochon, J., & Ramirez-Ruiz, E. 2011, *ApJ*, 737, 89
- Di Stefano, Voss, R., & Claeys, J.S.W. 2011, *ApJ*, 738, L1
- Folatelli, G., Phillips, M.M., Morrell, N., Tanaka, M., Maeda, K., Nomoto, K., et al. 2012, *ApJ*, 745, 74
- Guerrero, J., Garcis-Berro, E., & Isern, J. 2004, *A&A*, 413, 257
- Hachisu, I., Kato, M., Saio, H., & Nomoto, K. 2012, *ApJ*, 744, 69
- Hillebrandt, W., & Niemeyer, J. 2000, *ARAA*, 38, 191
- Ilkov, M., & Soker, N. 2012, *MNRAS*, 419, 1695
- Iwamoto, K., Nomoto, K., & Thielemann, F.-K.. 1999, *ApJS*, 54, 335
- Iben, I., Jr., & Tutukov, A. V. 1984, *ApJS*, 54, 335
- Justham, S. 2011, *ApJ*, 730, L34
- Kasen, D., Röpke, F., & Woosley, S. 2009, *Nature*, 460, 869
- Kamiya, Y., & Nomoto, K. 2011, in preparation
- Kato, M., Hachisu, I., Kiyota, S., & Saio, H. 2008, *ApJ*, 684, 1366
- Kawai, Y., Saio, H., & Nomoto, K. 1987, *ApJ*, 315, 229
- Livio, M. 2000, *Type Ia Supernovae: Theory and Cosmology* (Cambridge Univ. Press), 33
- Maeda, K., et al. 2010a, *ApJ*, 394, 239
- Maeda, K., et al. 2010b, *Nature*, 466, 82
- Nakasato, N., & Nomoto, K. 2003, *ApJ*, 588, 842
- Nakasato, N., & Nomoto, K. 2011, in preparation
- Nomoto, K. 1984, *ApJ*, 277, 791
- Nomoto, K. 1987, *ApJ*, 322, 206
- Nomoto, K., & Iben, I. Jr. 1985, *ApJ*, 297, 53
- Nomoto, K., Iwamoto, K., & Kishimoto, N. 1997, *Science*, 276, 1378
- Nomoto, K., Kamiya, Y., Nakasato, N., Hachisu, I., & Kato, M. 2009, in *AIPC 1111: Probing Stellar Populations out to the Distant Universe: Cefalu 2008* (AIP), 267
- Nomoto, K., & Kondo, Y. 1991, *ApJ*, 367, L19
- Nomoto, K., Sugimoto, D., & Neo, 1976, *Ap. Sp. Sci.*, 39, L37
- Nomoto, K., Thielemann, F.-K., & Yokoi, K. 1984, *ApJ*, 286, 644
- Nomoto, K., Umeda, H., Kobayashi, C., Hachisu, I., Kato, M., & Tsujimoto, T. 2000, in *AIPC 522: Cosmic Explosions*, ed. S. S. Holt & W. W. Zhang (AIP), 35 (astro-ph/0003134)
- Pakmor, R., et al. 2010, *Nature*, 463, 61
- Pakmor, R., et al. 2011, *Supernovae and their Host Galaxies*, Sydney 2011
- Parrent, J.T., et al. 2011, *ApJ*, 732, 30
- Rosswog, S., Davis, M.B., Thielemann, F.-K., & Piran, T. 2000, *A&A*, 360, 171
- Saio, H., & Nomoto, K. 1985, *A&A*, 150, L21
- Saio, H., & Nomoto, K. 1998, *ApJ*, 500, 388
- Segretain, L., Chabrier, G., & Mochkovitch, R. 1997, *ApJ*, 481, 355
- Shen, K., & Bildsten, L. 2007, *ApJ*, 660, 1444
- Shen, K., Bildsten, L., Kasen, D., & Quataert, E. 2012, *ApJ*, 748, 35
- Shigeyama, T., Nomoto, K., Yamaoka, H. & Thielemann, F.-K. 1992, *ApJ*, 386, L13
- Shioya, T., Sano, T., & Takabe, H. 2007, *PASJ*, 59, 753
- Timmes, F.X., & Swesty, F.D. 2000, *ApJS*, 126, 501
- Uenishi, T., Nomoto, K., & Hachisu, I. 2003, *ApJ*, 595, 1094
- Usuda, T., Krause, O., Tanaka, M., Hattori, T., Goto, M., Birkmann, S.M., & Nomoto, K. 2011, in these Proceedings
- Webbink, R. F. 1984, *ApJ*, 277, 355
- Yoon, S.-C., & Langer, N. 2004, *A&A*, 419, 623
- Yoon, S.-C., Podsiadlowski, Ph., & Rosswog, S. 2007, *MNRAS*, 380, 933